NANO LETTERS

2008
Vol. 8, No. 2
647−651

Measuring the Work Function of Carbon Nanotubes with Thermionic Method

Peng Liu,* Qin Sun, Feng Zhu, Kai Liu, Kaili Jiang, Liang Liu, Qunqing Li, and Shoushan Fan

Department of Physics and Tsinghua-Foxconn Nanotechnology Research Center, Tsinghua University, Beijing 100084, China

Received November 26, 2007

ABSTRACT

The work function of carbon nanotubes might depend on their diameters and the number of walls, and be different for their tips and sidewalls. Here we report the work function measurement of single-walled, double-walled, and multiwalled carbon nanotubes by investigating the thermionic emission from the middle of their bundles. It is found that the sidewall work functions of the three kinds of carbon nanotubes are all around 4.7–4.9 eV; the diameter and the numbers of walls have no obvious influence on their work functions. For the carbon nanotube bundle with some tips appearing in the middle, the measured work function is smaller than without tips, indicating that the work function of tips is smaller than that of the sidewalls. This tip effect also results in a difference in the thermionic emission characteristic, implying non-uniform work function distribution along the bundle.

Work function is an important parameter of carbon nanotubes (CNTs) for its many different kinds of interesting applications. The applications on nanoelectrics will be focused on the sidewall work function because it will decide the contact properties with the foreign materials and influence the performance of devices. Applications on field emission will be focused on the work function of tips because the electrons emitted from there. There are a lot of measurements and calculations of the work function of CNTs with different methods;[1−16] we have also measured the work function of multiwalled CNT (MWCNT) yarns with the thermionic emission method,[17] which has advantages such as accurate measurement and automatic elimination of adsorbates, etc. However, there are still some experimental issues that need to be clarified. The first one is the relations between work function and the diameter or number of walls of CNTs. Although there are also some theoretical predictions,[1−3] experimental verification is still needed. Another concern of the experimental work function measurement is the difference of the sidewall and tips. Theoretical calculations[4] have shown that the work functions of tips and the sidewall are different, but the accurate experimental measurement for each of them separately is still scarce. The experimental difficulty lies in that the CNTs are usually entangled together. The work functions of tips and sidewalls are difficult to separate.

In this paper, with the thermionic emission method, we measured the work function of the single-walled CNTs (SWCNTs), double-walled CNTs (DWCNTs), and MWCNTs. The samples are all the CNT bundles synthesized with the chemical vapor deposition (CVD) on a silicon wafer with a patterned catalyst island. We have controlled the synthesis process to alleviate the effects of tips along the bundle. Therefore the work function of sidewalls can be measured separately. We at first discussed the relation between work function and diameter and the number of walls of CNTs in this experiment. To study the work function of the tips, we have further investigated the thermionic emission of the CNT bundles with some tips along them which is also realized by controlling the synthesis condition. The work function difference between the tips and sidewalls is discussed.

The measured sidewall work functions of SWCNTs, DWCNTs, and MWCNTs are around 4.7−4.9 eV. This result shows that the diameter or number of walls has no obvious influence on the work function of the CNTs in our experiment. The study about the tips shows that their work function is smaller than that of the sidewalls. It is in accordance with our previous work function measurement for the MWCNT yarns.

The CNT samples are all the bundles picked out from the CNT arrays synthesized with a CVD method on the silicon wafer with patterned catalyst islands. Figure 1a−c show their scanning electron microscope (SEM) images from the top view.

The height of the CNT bundles is around 400−600 μm. Therefore, the electrode structures with conventional size will not be suitable to study their thermionic emission. We have designed the microelectrode structures as shown in Figure 2.

* To whom correspondence should be addressed: Telephone: 8610-62794280. Fax: 8610-62792457. E-mail: Liup01@mails.thu.edu.cn.

10.1021/nl0730817 CCC: $40.75
Published on Web 01/29/2008

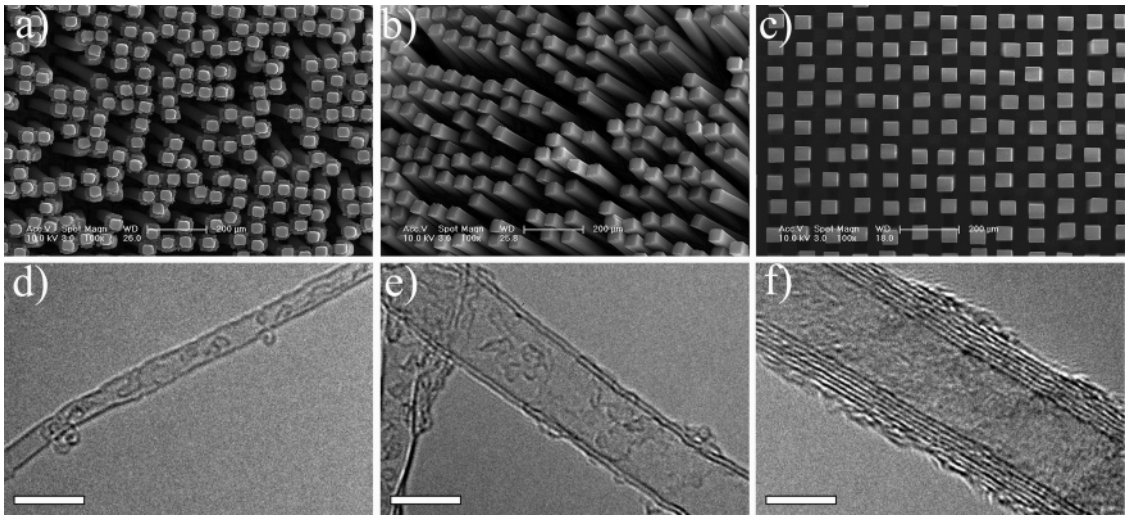

Figure 1. SEM images (top view) of (a) SWCNT, (b) DWCNT, and (c) MWCNT arrays synthesized with the CVD method; (d−f) typical transmitted electron microscope (TEM) images of the SWCNT, DWCNT, and MWCNT samples in our experiment, respectively. The scale bars in the TEM images are all 5 nm.

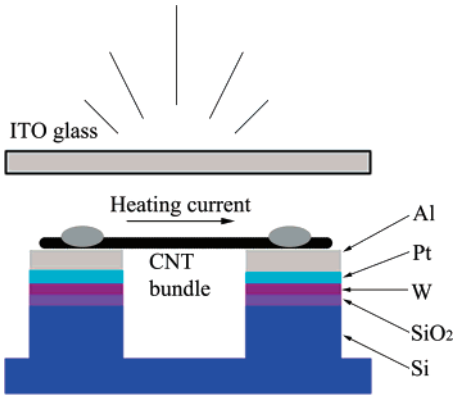

Figure 2. Schematic electrode structure to measure the sidewall work function of CNTs.

The electrode structure was formed on the silicon wafer with the SiO_2 layer. We at first defined the electrode patterns with a photoresist by lithography technologies (EVG 620), and then the metal electrode layers were electron-beam evaporated onto the wafer (Anelva L-400EK). A lift-off process was adopted to remove the resist after that. At last, a dry etching process was performed (Anelva Helicon DFR) to form the trench. The CNT bundles were then welded on the electrodes with a wire bonder (Kulicke and Soffa 4523). The metal layer of W is to improve the adhesion between wafer and electrode materials, and the Al layer serves as the resist layer in the dry etching process and improves the welding property of the electrode at the same time. The trench is designed to suspend the CNT bundles to reduce the thermal dissipation during the heating.

Figure 3a−c show the SEM images of the SWCNT, DWCNT, and MWCNT bundles bonded on the electrode structures. As we have mentioned, it is important to exclude the tip effects in the work function measurement for the sidewalls. According to our synthesis experiments, usually there will be some CNTs which stopped growth earlier than the others and their tips will appear along the bundle as a result. However, this process usually happened a little while after the growth starts; therefore if we choose the part of bundles near the starting end for research, the tip effects can be alleviated. For SWCNT and DWCNT samples, we have chosen the part near the starting ends to study, which is shown in Figure 3a and b. The thin ends are the bottom ends (the stopping end in the bottom growth mode[18,19]), and the bundle diameters between the two electrodes are uniform. For the MWCNT bundles, we have stopped the growth intentionally a little while later after the growth started so that there are still not many tips appearing. The insets in Figure 3a−c show that the edge of the bundle is uniform and there are no tips along them.

The CNT bundles were heated in a vacuum chamber at the base pressure of 2×10^{-5} Pa with a source meter at the DC mode (Keithley 2410). Figure 3d−f are the incandescence images of the SWCNT, DWCNT, and MWCNT bundles. We can find that they are mostly heated in the middle part. It shows that there is no large difference for the resistance along the bundle, and the CNT density along the bundle is uniform. The thermionic emission current was collected by an indium tin oxide (ITO) glass anode with another source meter (Keithley 237). The incandescence light transmitted from the ITO glass was collected by a spectro-radiometer (Konica-Minolta CS 1000A) with a small area lens (CS 1000S) and was fit with the black body emission[17,20] to calculate the temperatures.

The work function was calculated according to Richardson's formula,[21]

$$j_0 = AT^2 \exp\left(-\frac{\phi}{kT}\right)$$

where j_0 is the zero field thermionic emission current density, A is Richardson's emission constant, T is the absolute temperature, ϕ is the work function of the cathode at absolute zero temperature, k is the Boltzmann constant.

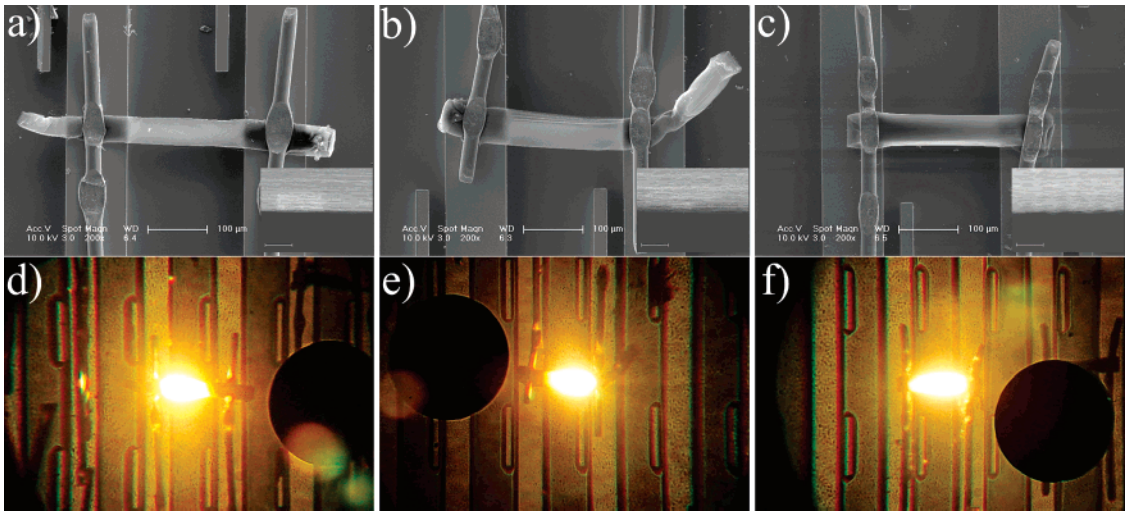

Figure 3. (a−c) SEM images of SWCNT, DWCNT, and MWCNT bundles bonded on the microelectrodes, respectively; insets in a−c are their enlarged SEM images at the edges of the bundles. (d−f) Their corresponding incandescence images.

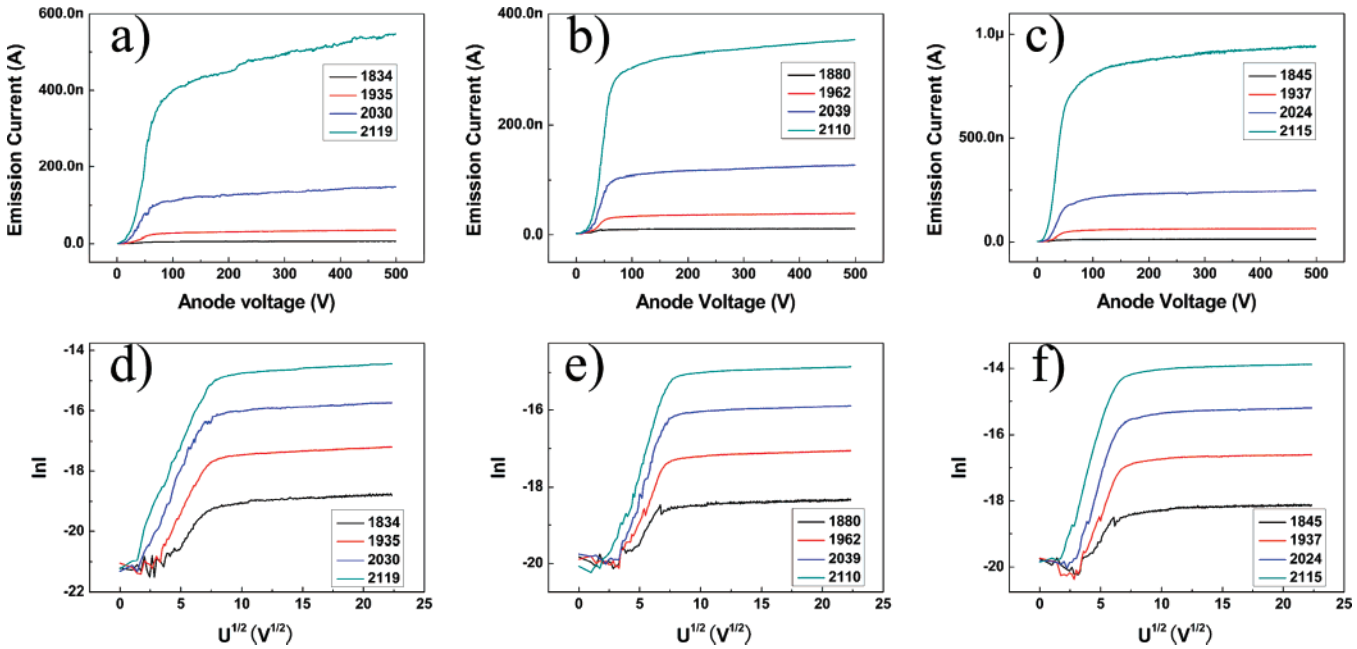

Figure 4. (a−c) Thermionic *IV* curves and (d−f) the $\ln I - \sqrt{V}$ curves of SWCNT, DWCNT, and MWCNT bundles shown in Figure 3, respectively. The label of each curve shows the corresponding temperature of the bundles in Kelvin.

The "zero field thermionic emission current" j_0 can be calculated from the *IV* curves according to the Schottky effect,[22]

$$j_a = j_0 \exp\left(-\frac{e\sqrt{eE/4\pi\epsilon_0}}{kT}\right)$$

where j_a is the thermionic emission current density, e is the electron charge, E is the electric field on the thermionic cathode surface, and ϵ_0 is the vacuum dielectric constant. E can be substituted by $\alpha\sqrt{U_a+U_c}$. Here α is a constant determined by the geometry of electrode structures, U_a is the anode voltage in volts, U_c is the contact potential between the cathode and anode, which is usually below 1 V and can be neglected in the calculation. According to the data recorded by Keithley 237, j_0 can be easily derived. Figure 4 shows the *IV* and $\ln I - \sqrt{V}$ curves of the SWCNT, DWCNT, and MWCNT samples shown in Figure 3.

We have measured three samples for each of the three kinds of CNT bundles. The measured work functions are listed in Table 1.

The work function is very close to the values measured by the photoemission method in refs 6 and 7. It is easy to understand because the photoemitted electrons for the samples in refs 6 and 7 are also mostly come from the sidewalls. The diameters of the SWCNT, DWCNT, and MWCNT measured from the TEM images are respectively 2.2 ± 0.8 nm, 4.9 ± 0.8 nm, and 8.7 ± 1.7 nm, and the number of walls are 1, 2, and 4−7. Although the diameter or number of walls of the SWCNT, DWCNT, and MWCNT

Table 1. Work Function of CNT Bundles

sample number	temerature range (K)	work function (eV)	type
1	1826−2128	4.70 ± 0.03	SWCNT
2	1874−2136	4.89 ± 0.02	SWCNT
3	1817−2129	4.92 ± 0.03	SWCNT
4	1880−2148	4.85 ± 0.03	DWCNT
5	1865−2151	4.85 ± 0.01	DWCNT
6	1846−2092	4.87 ± 0.05	DWCNT
7	1826−2115	4.91 ± 0.03	MWCNT
8	1808−2088	4.80 ± 0.03	MWCNT
9	1747−2100	4.82 ± 0.04	MWCNT

varied, their work functions are still very close. It shows that the diameter or number of walls have no obvious influences on the work function of the CNTs in our experiment. This result is also in accordance with the theoretical calculations in refs 1 and 2 which show that the work function of CNTs will approach the same value when their diameters are larger than 1 nm. The diameters of our samples are all beyond this limit. This conclusion is easy to understand because the graphite layers of CNTs will exhibit the same property when the curvature effect become minus.

To study the tip effect on the work function of CNT bundles, we have also synthesized the CNT bundles with some tips appearing along the bundle. By allowing the CNT bundles to naturally grow to death, there will be some tips appearing along the bundle due to some CNTs which stopped growth earlier. We have investigated the thermionic emission characteristics of of this kind of CNT bundles. Figure 5a shows the SEM images of the MWCNT bundles which has naturally stopped growth. Under the bottom growth mode,[18,19] the CNTs at the bottom end is more sparse and disorderd than those at the top end, as shown in Figure 5c and d. Therefore, when they were heated with current, the bottom end will be much hotter and brighter than the top end as Figure 5b has shown for its higher resistance. The thermionic emission current from the samples will be the mixture from the tips and sidewalls.

Figure 6 is the thermionic emission *IV* curves of the CNT bundle. The work function calculated from thermionic emission data is 4.41 ± 0.03 eV, which is smaller than that of the sidewall. Our previous measurements for the MWCNT yarns also give a smaller work function than the sidewalls. It strongly shows that the work function of CNT tips is lower than that of the sidewalls. The difference in work functions of tips and sidewalls may originate from their different electronic structures and image potentials. Zhou et al. have discussed the influence of the different electronic structures of tips and sidewall.[4] Furthermore, because the tips and sidewalls have different atomic and geometric structures, the image potential of an emitted electron felt at the tips and sidewall will also be different, which can also induce the work function difference of the tips and sidewalls.

The thermionic *IV* curves of the bundle with tips are also different from that without tips. The transition points from the "retarding field regime" to the "accelerating field

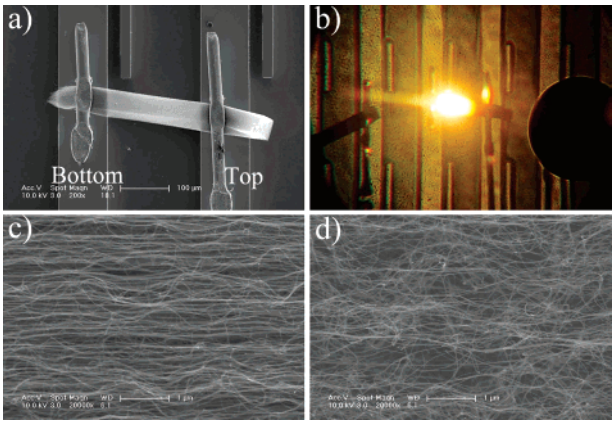

Figure 5. (a) SEM images of the MWCNT bundles which stopped growth naturally; (b) the incandescence images of the bundle; (c and d) the enlarged SEM image of the top and bottom ends.

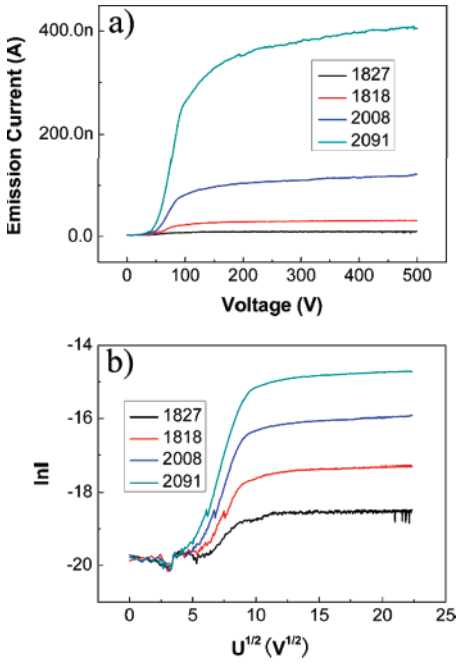

Figure 6. (a and b) Thermionic *IV* and ln $I - \sqrt{V}$ curves of the sample shown in Figure 5. The label of each curve shows the corresponding temperature of the bundles in Kelvin.

regime"[22] in the ln $I - \sqrt{V}$ curves in Figure 4 are all ~7 on the horizontal axis (50 V in the *IV* curves), while the transition point in Figure 6 is at ~9 on the horizontal axis (80 V in the *IV* curves). According to the thermionic emission theories,[23] it can be interpreted by the "patch field" effect which is shown in Figure 7.

If the work function on the cathode surface is not uniform, there will be the contact potential and the "self-constructed field". The anode voltage have to neutralize this electric field first before drawing out the thermionic electrons. Therefore the transition voltage from retarding field regime to accelerating field regime is increased for CNT bundles with non-uniform work function distribution.

In conclusion, we have reported the measurement of the work function of SWCNT, DWCNT, and MWCNT bundles with thermionic methods in this paper. The work functions

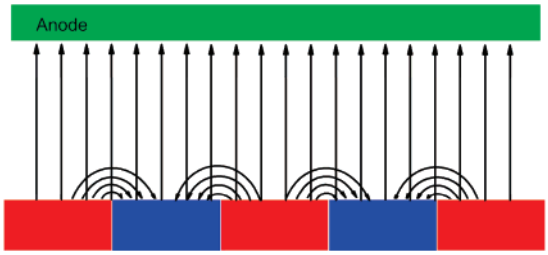

Figure 7. "Patch field" effect induced by the nonuniformity of the work function on the cathode surface. The arrow is the direction of force on electrons. The red part is the low work function region.

of the sidewall of SWCNTs, DWCNTs, and MWCNTs are around 4.7−4.9 eV. The diameter or the numbers of walls have no obvious influence on the work function of CNTs in our experiments. The tips show a smaller work function than the sidewalls. The result is in accordance with other experiment measurements and theoretical calculations. It is hoped the result will be useful for the application and theoretical research of the CNTs.

Acknowledgment. This work is financed by the National Basic Research Program of China (2005CB623606) and NSFC (10334060).

References

(1) Zhao, J.; Han, J.; Lu, J. P. *Phys. Rev. B* **2002**, *65*, 193401.
(2) Shan, B.; Cho, K. *Phys. Rev. Lett.* **2005**, *94*, 236602.
(3) Shan, B.; Cho, K. *Phys. Rev. B* **2006**, *73*, 081401(R).
(4) Zhou, G.; Duan, W.; Gu, B. *Phys. Rev. Lett.* **2001**, *87*, 095504.
(5) Ago, H.; Kugler, T.; Cacially, F.; Petritsch, K.; Friend, R. H.; Salaneck, W. R.; Ono, Y.; Yamabe, T.; Tanaka, K. *Synth. Met.* **1999**, *103*, 2494.
(6) Shiraishi, M.; Ata, M. *Carbon* **2001**, *39*, 1913.
(7) Suzuki, S.; Bower, C.; Watanabe, Y.; Zhou, O. *Appl. Phys. Lett.* **2000**, *76*, 4007.
(8) Suzuki, S.; Watanabe, Y.; Homma, Y.; Fukuba, S.; Heun, S.; Locatelli, A. *Appl. Phys. Lett.* **2004**, *85*, 127.
(9) Cui, X.; Freitag, M.; Martel, R.; Brus, L.; Avouris, P. *Nano Lett.* **2003**, *3*, 783.
(10) Gao, R.; Pan, Z.; Wang, Z. L. *Appl. Phys. Lett.* **2001**, *78*, 1757.
(11) Fransen, M. J.; van Rooy, T. L.; Kruit, P. *Appl. Surf. Sci.* **1999**, *146*, 312.
(12) Gröning, P.; Nilsson, L.; Ruffieux, P.; Clergereaux, R.; Gröning, O. In *Encyclopedia of Nanoscience and Nanotechnology*; Nalwa, H. S., Ed.; American Scientific Publishers: Stevenson Ranch, CA, 2004; Vol. 1, pp 547−579.
(13) Gröning, O.; Küttel, O. M.; Emmenegger, C.; Gröning, P.; Schlapbach, L. *J. Vac. Sci. Technol. B* **2000**, *18*, 665.
(14) Sinitsyn, N. I.; Gulyaev, Y. V.; Torgashov, G. V.; Chernozatonskii, L. A.; Kasakovskaya, Z. Y.; Zakharchenko, Y. F.; Kiselev, N. A.; Musatov, A. L.; Zhbanov, A. I.; Mevlyut, S. T., et al. *Appl. Surf. Sci.* **1997**, *111*, 145.
(15) Obraztsov, A. N.; Volkov, A. P.; Pavlovsky, I. *Diamond Relat. Mater.* **2000**, *9*, 1190.
(16) Dean, K. A.; von Allmen, P.; Chalamala, B. R. *J. Vac. Sci. Technol. B* **1999**, *17*, 1959.
(17) Liu, P.; Wei, Y.; Jiang, K.; Sun, Q.; Zhang, X.; Fan, S.; Zhang, S.; Ning, C.; Deng, J. *Phys. Rev. B* **2006**, *73*, 235412.
(18) Liu, L.; Fan, S. *J. Am. Chem. Soc.* **2001**, *123*, 11502.
(19) Liu, K.; Jiang, K.; Feng, C.; Chen, Z.; Fan, S. *Carbon* **2005**, *43*, 2850.
(20) Li, P.; Jiang, K.; Liu, M.; Li, Q.; Fan, S. *Appl. Phys. Lett.* **2003**, *82*, 1763.
(21) Richardson, O. W. *The emission of electricity from hot bodies*, 2nd ed; Longmans, Green and Co. 10: London, 1921; Chapter 2, pp 29−59.
(22) Reimann, A. L. *Thermionic Emission*; John Wiley and Sons, Inc.: New York, 1934; Chapter 1, p 61.
(23) Herring, C.; Nichols, M. H. *Rev. Mod. Phys.* **1949**, *21*, 185.

NL0730817